*crystals*

**MDPI**

*Article*

# Tilkerodeite, Pd$_2$HgSe$_3$, a New Platinum-Group Mineral from Tilkerode, Harz Mountains, Germany

**Chi Ma** [1,*] **, Hans-Jürgen Förster** [2] **and Günter Grundmann** [3]

1    Division of Geological and Planetary Sciences, California Institute of Technology, Pasadena, CA 91125, USA
2    Helmholtz Centre Potsdam German Research Centre for Geosciences GFZ, D-14473 Potsdam, Germany; forhj@gfz-potsdam.de
3    Eschenweg 6, D-32760 Detmold, Germany; grundmann.g@gmx.de
*    Correspondence: chima@caltech.edu

check for updates

**Abstract:** Tilkerodeite, ideally Pd$_2$HgSe$_3$, is a new platinum-group selenide from the Eskaborner Stollen (Adit Eskaborn) at Tilkerode, Harz Mountains, Germany. Tilkerodeite crystals occur as euhedral inclusions in tiemannite or as extremely fine-grained lamellar aggregates (grain-size up to 3 μm) in a dolomite–ankerite matrix, together with clausthalite, tiemannite, jacutingaite, stibiopalladinite, and native gold. Neighbouring Se-bearing minerals include tischendorfite and chrisstanleyite. Tilkerodeite is opaque with a metallic luster, and is flexible in blade-like crystals, with perfect basal cleavage {001}. In plane-polarized light, tilkerodeite is brownish-grey. It is weakly bireflectant, and weakly pleochroic in shades of light-brown and grey. The anisotropy is weak, with rotation tints in weak shades of greenish-brown and grey-brown. The range of reflectance is estimated in comparison to clausthalite with 45–50%. Electron-microprobe analyses yield the mean composition (wt. %) Se 32.68, Hg 26.33, Pt 20.62, Pd 15.89, Pb 2.72, Cu 0.66, S 0.27, total 99.17 wt. %. The empirical formula (based on six atoms *pfu*) is (Pd$_{1.08}$Pt$_{0.76}$Pb$_{0.09}$Cu$_{0.07}$)$_{\Sigma2.00}$Hg$_{0.95}$(Se$_{2.98}$S$_{0.07}$)$_{\Sigma3.05}$. The ideal formula is Pd$_2$HgSe$_3$. Tilkerodeite is trigonal, with Pt$_4$Tl$_2$Te$_6$-type structure, space group $P\bar{3}m1$, $a$ = 7.325(9) Å, $c$ = 5.288(6) Å, $V$ = 245.7(9) Å$^3$, and $Z$ = 2. It is the Pd-analogue of jacutingaite. Tilkerodeite formed hydrothermally, possibly involving the alteration of tiemannite by low-temperature oxidizing fluids. The new species has been approved by the IMA-CNMNC (2019-111) and is named after the locality. Tilkerode is the most important selenide-bearing occurrence in Germany and type locality of naumannite, eskebornite, and tischendorfite.

## 1. Introduction

Tilkerode, in the eastern Harz Mountains, is the most important selenide deposit in Germany, which was mined for iron (hematite) and native gold in the 18 and 19 Centuries [1]. It hosts 18 confirmed selenides, and is the type locality for naumannite (Ag$_2$Se), eskebornite (CuFeSe$_2$), and tischendorfite (Pd$_8$Hg$_3$Se$_9$) [2].

This paper provides the description of a new platinum-group element (PGE) mineral, tilkerodeite, ideally Pd$_2$HgSe$_3$, from Tilkerode. The new selenide was discovered as part of the re-examination of the tischendorfite co-type material (14 newly mounted and polished thick sections taken from veinlet sample No. 4154, Figure 1) and studied by polarized light microscopy (PLM), scanning electron microscopy (SEM) combined with electron-probe microanalyses (EPMA), and electron back-scatter diffraction (EBSD). This sample was collected from the Eskaborner Stollen (Eskaborn adit; 51°38′3″ North, 11°19′4″ East), at the 60-m level, 5 m north of the blind shaft IV [1].

The new species and its name have been approved by the Commission on New Minerals, Nomenclature and Classification (CNMNC) of the IMA, proposal n. 2019–111. The holotype polished section is housed in the Mineral Collection at the Mineralogical Institute of the Technische Universität Bergakademie Freiberg, Freiberg, Germany, under the inventory Number MiSa84670. The mineral name is for the locality.

## 2. Materials and Methods

Tilkerodeite was studied for appearance and optical and physical properties by polarized light microscopy (PLM). The tilkerodeite-containing sample was prepared for optical microscopy using standard diamond polishing techniques. Sample preparation involved the following machinery and materials: lapping and polishing machine type "Buehler Metaserv", Buehler UK Ltd., Coventry, UK; grinding and polishing machine type "Kent MK 2A", Engis Ltd., UK; "Pellon" polishing chemotextile type PAN-W, Hartfeld & Co., Allerød, Denmark; diamond suspension, water soluble (grain sizes 6 μm, 3 μm, 1 μm, 0.25 μm) type Gala-Tec GmbH, Kaiserslautern, Germany; and fixed abrasive steel discs, consisting of diamond in steel-binding (grain sizes 600, 800, 1200 mesh). Optical studies were performed using a "Leitz DMRM" polarizing microscope, Type 301-371-010, Leitz/Leica, Wetzlar, Germany (air-objectives: PL Fluotar 50×, aperture 0.85 BD; PL APO 100×, aperture 0.90 BD; PL APO 150×, aperture 0.90 D). Digital photomicrographs were taken using a CANON EOS 70D camera mounted on the microscope.
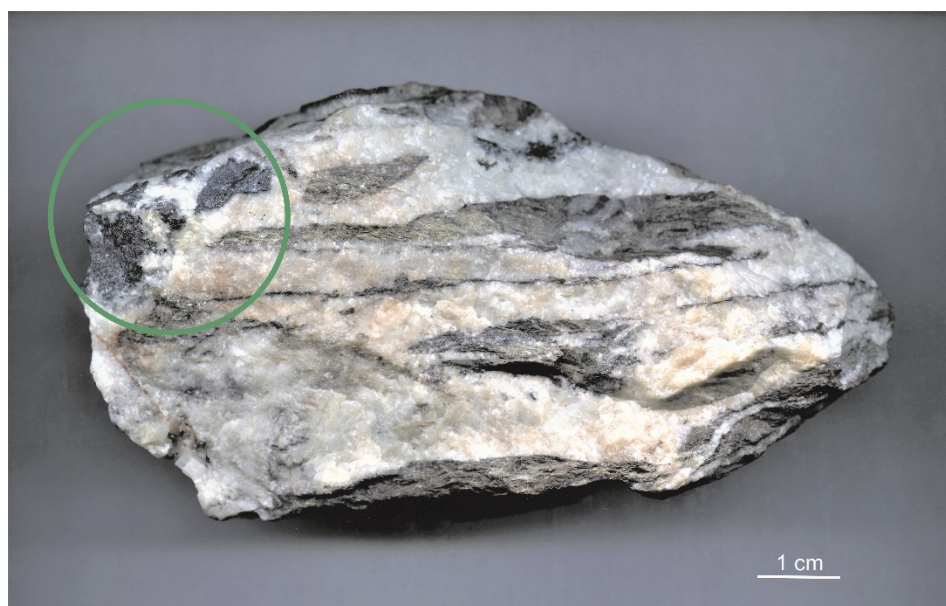


**Figure 1.** Cross section through Tilkerode sample No. 4154, the co-type specimen of the tischendorfite- and chrisstanleyite-bearing dolomite/ankerite veinlet (partially reddish stained by hematite), which forms a typical rubble breccia. The position of the gold-bearing Pt–Pd–Hg–Pb–Sb–Se mineralization is marked by a green circle. Width of image 12 cm.

EPMA, high-resolution SEM, and EBSD were used to characterize the composition and structure of the new mineral and associated phases. Back-scatter electron (BSE) imaging was performed using a ZEISS 1550VP field emission SEM. EBSD analyses were performed using an HKL EBSD system on the ZEISS 1550VP SEM, operated at 20 kV and 6 nA in focused-beam mode with a 70° tilted stage and a variable pressure mode (25 Pa) using procedures described in Ma and Rossman (2008, 2009) [3,4]. The focused electron beam is several nanometers in diameter. The spatial resolution for diffracted backscatter electrons is ~30 nm in size. The EBSD system was calibrated using a single-crystal silicon standard. The structure was determined and cell constants were obtained by

matching the experimental EBSD patterns with structures of $Pd_2HgSe_3$, $Pt_2HgSe_3$, other Pd–Hg–Se, and Pt–Hg–Se phases. Quantitative wavelength-dispersive (WDS) elemental microanalysis was performed using a JEOL 8200 electron microprobe (10 kV and 10 nA, focused beam). The focused electron beam was ~120 nm in diameter. Analyses were processed with the CITZAF correction procedure [5]. Mineral identification was also made by semi-quantitative energy-dispersive (EDS) elemental analysis using a JEOL 8230 electron microprobe.

## 3. Results

### 3.1. Appearance

The selenides and native gold occur in a dolomite/ankerite vein, filling fractures and cementing an older, strongly fragmented dolomite generation in a rubble breccia (Figure 1).

Tilkerodeite forms thin tabular or spindle-shaped crystals (up to 3 μm in length and 0.5 μm in width); intersertal intergrowth with clausthalite (PbSe) and tiemannite (HgSe); and, more rarely, stibiopalladinite ($Pd_5Sb_2$), jacutingaite ($Pt_2HgSe_3$), and native gold (Figures 2–5). Tilkerodeite crystals of this association were studied for composition and structure. In the immediate vicinity of this type of mineral assemblage occur tiemannite–(clausthalite) aggregates (of up to 2 mm in diameter), which contain large quantities of tiny, oriented lamellae of what have been identified by EPMA-EDS representing both tilkerodeite and jacutingaite (Figure 6). These aggregates have concave bulges towards the adjacent dolomite, which show distinct corrosion features. This type of inclusion-rich tiemannite is partially replaced by dolomite and/or clausthalite.
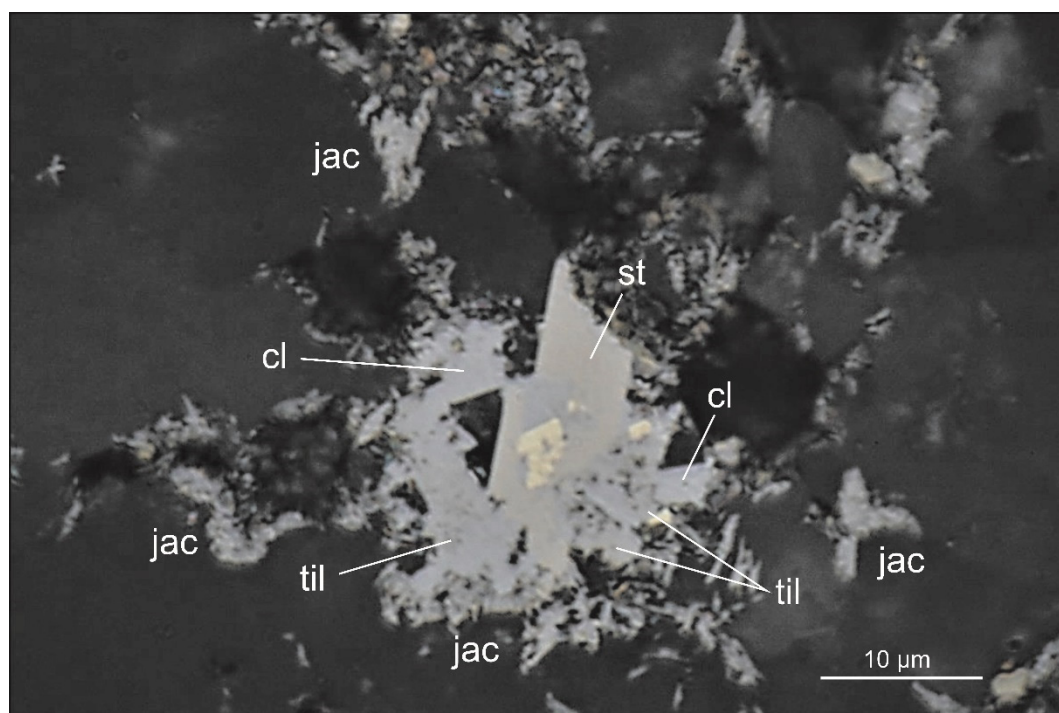


**Figure 2.** Reflected plane-polarized light digital image in air showing tilkerodeite (til, crème-grey) with clausthalite (cl, light-grey), jacutingaite (jac, crème-grey), native gold (light-yellow), and stibiopalladinite (st, light crème-brown), in dolomite matrix (dark-grey). Width of image 75 μm.

### 3.2. Physical and Optical Properties

Tilkerodeite is black or grey in color and possesses a black streak. It is opaque in transmitted light, exhibiting a metallic lustre. It is characterized by a distinct basal cleavage and parting parallel {001}. The mineral is flexible, with distinct layered structure, forming laminated crystals that are partially

curved. Cathodoluminescence was not observed. The relative polishing hardness of tilkerodeite in comparison to clausthalite is estimated to ~3 Mohs.

Magnetic properties and density could not be measured owing to small grain size. Calculated density is 9.67 g·cm$^{-3}$, considering the empirical formula and EBSD unit-cell data reported in Sections 3.3 and 3.4.
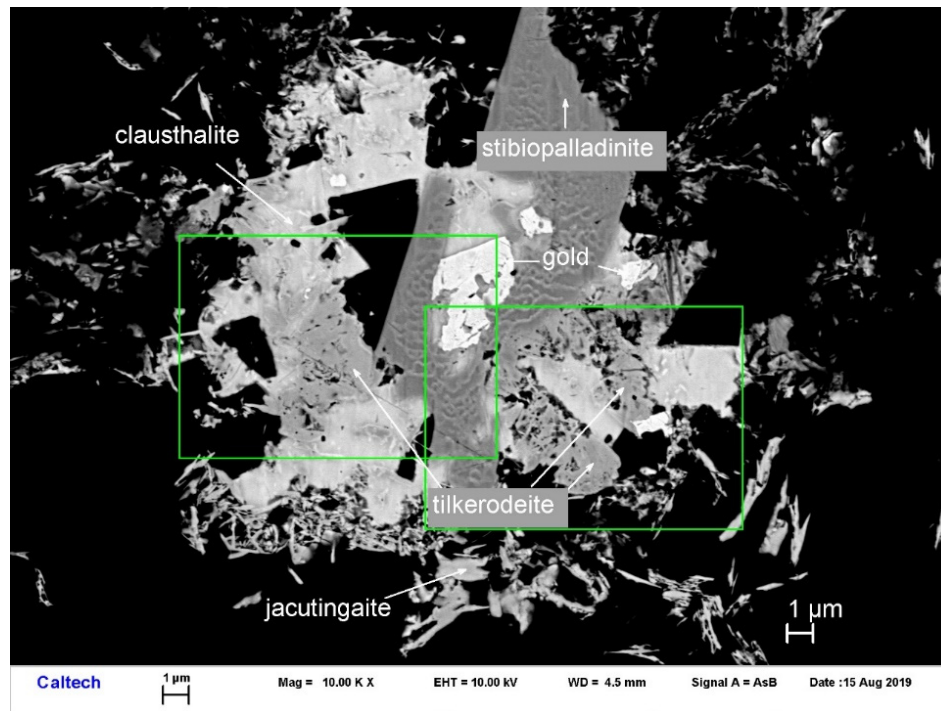


**Figure 3.** SEM-back-scattered electron (BSE) image of the mineral aggregate shown in Figure 2. Areas enclosed by green rectangles are shown in Figures 4 and 5.
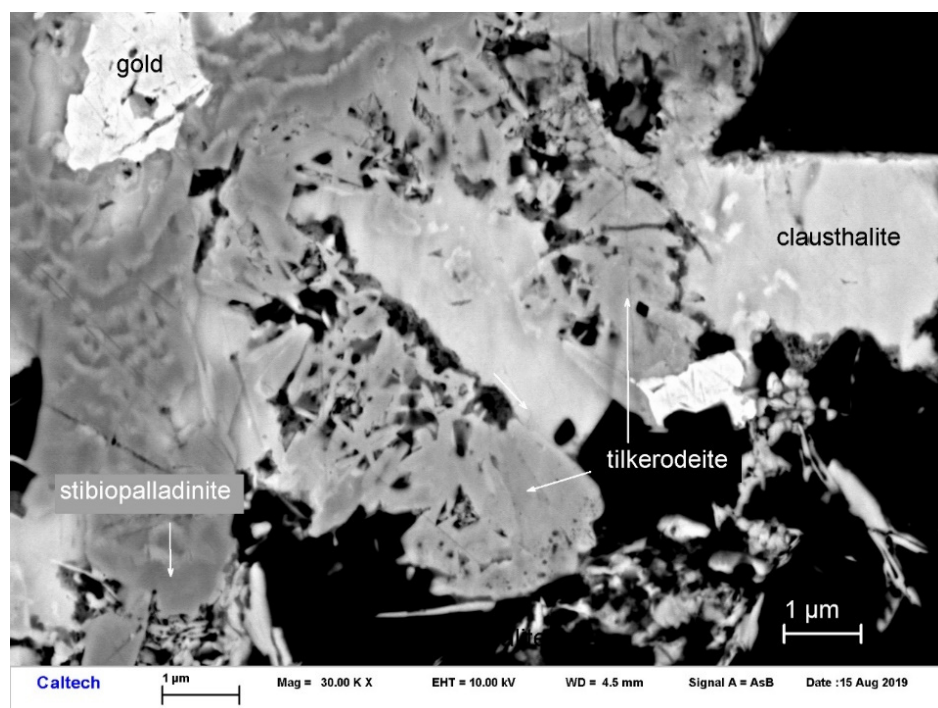


**Figure 4.** SEM-back-scatter electron (BSE) image of the area shown in the right rectangle in Figure 3.
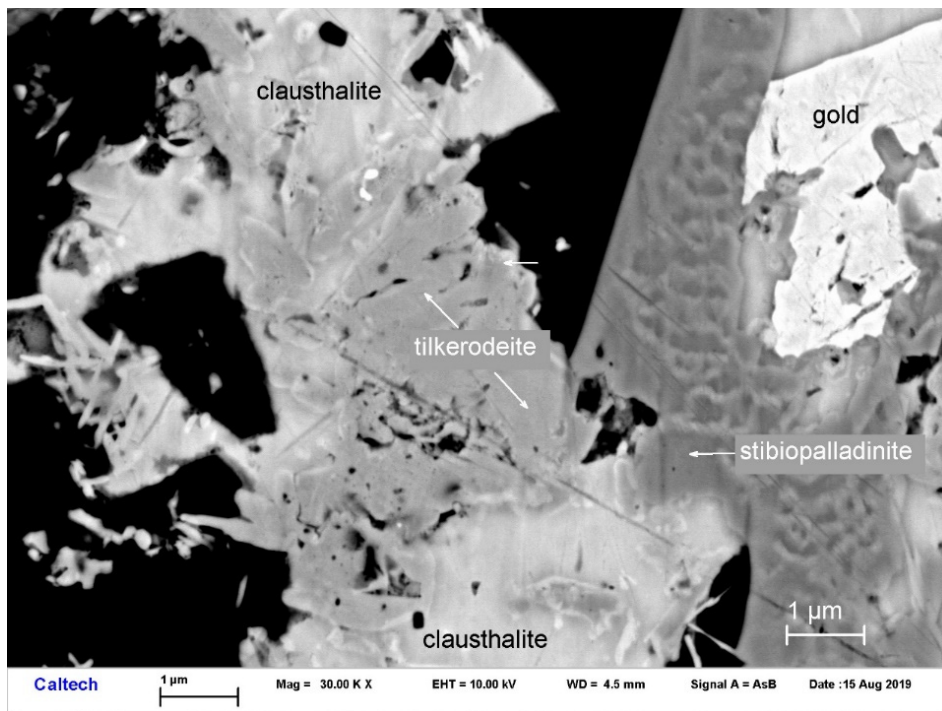
**Figure 5.** SEM-BSE image of the area shown in the left rectangle in Figure 3.

In plane-polarized incident light, tilkerodeite is brownish-grey to greyish-white. In the assemblage with clausthalite, it is weakly bireflectant, and weakly pleochroic in shades of brown and grey (Figure 2). The anisotropy is weak, with rotation tints in weak shades of greenish-brown and grey-brown.
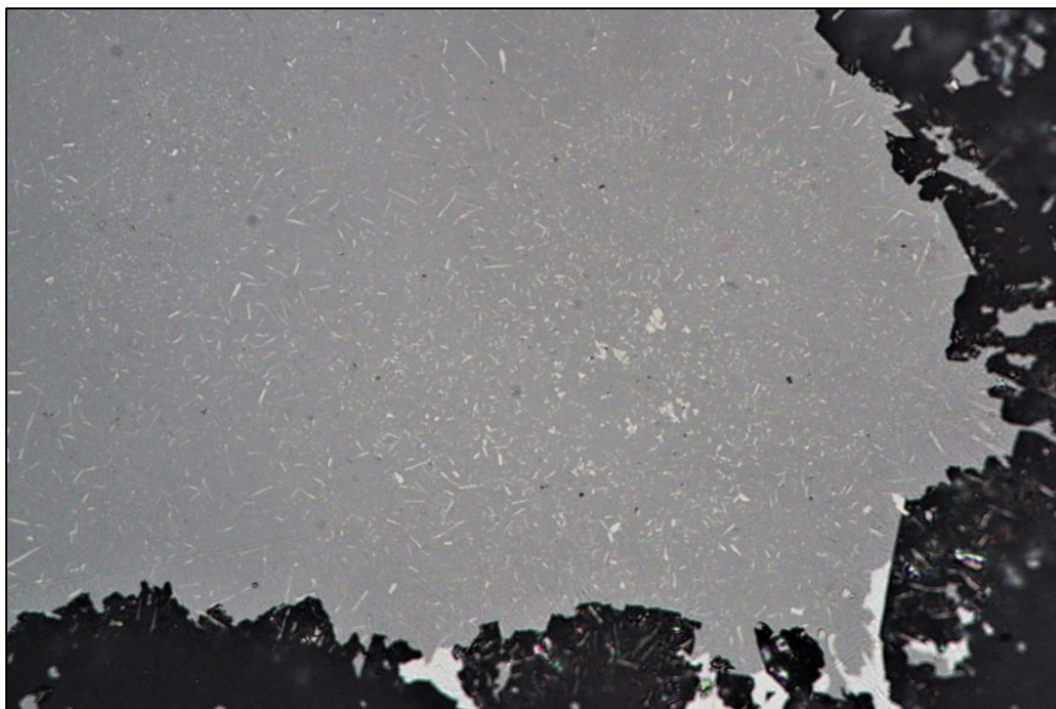


**Figure 6.** Reflected plane-polarized light digital image in air of a tiemannite–clausthalite aggregate containing a plethora of tiny, partly oriented lamellae of tilkerodeite and jacutingaite. The tiemannite grain shows concave bulges towards the adjacent dolomite, and is partially replaced by clausthalite (whitish-grey on the lower rim). Width of image 200 μm.

Quantitative reflectance values could not be acquired due to grain-size restrictions. The range of relative reflectance for tilkerodeite was estimated in comparison to clausthalite to 45–50%. Tilkerodeite has a slightly lower reflectance compared to neighboring jacutingaite, likely related to its comparatively larger Pd concentrations.

### 3.3. Chemical Composition

Table 1 compiles the analytical data for tilkerodeite (means of five spot analyses; ranges, 1δ standard deviations (SD); and probe standards).

**Table 1.** Chemical data for tilkerodeite.

| Constituent (wt. %) | Mean | Range | SD | Probe Standard |
|---|---|---|---|---|
| Pd | 15.89 | 15.31–16.33 | 0.40 | Pd |
| Pt | 20.62 | 20.37–20.98 | 0.24 | Pt |
| Pb | 2.72 | 1.73–3.32 | 0.65 | PbS |
| Cu | 0.66 | 0.56–0.84 | 0.11 | Cu |
| Hg | 26.33 | 25.27–27.06 | 0.72 | HgTe |
| Se | 32.68 | 32.21–33.04 | 0.31 | Se |
| S | 0.27 | 0.26–0.30 | 0.02 | PbS |
| Total | 99.17 | 98.51–99.75 | 0.52 | |

The mean chemical composition of type tilkerodeite is (wt. %) Se 32.68, Hg 26.33, Pt 20.62, Pd 15.89, Pb 2.72, Cu 0.66, S 0.27, and sum 99.17. Considering structural data for jacutingaite [6], small quantities of Pb and Cu are probably substituting for the platinum-group elements (PGE). Insignificant S is replacing for Se. The empirical formula (based on 6 atoms *pfu*) is $(Pd_{1.08}Pt_{0.76}Pb_{0.09}Cu_{0.07})_{\Sigma 2.00}$ $Hg_{0.95}(Se_{2.98}S_{0.07})_{\Sigma 3.05}$. The simplified formula is $(Pd,Pt)_2HgSe_3$. The ideal formula is $Pd_2HgSe_3$, which requires Pd 32.72, Hg 30.85, Se 36.43, total 100 wt. %.

### 3.4. Crystal Structure

Grain size of the new mineral was too tiny to permit extraction of a fragment for conventional single-crystal X-ray analysis. However, main parameters of crystal structure could be definitely resolved by EBSD. The EBSD patterns of tilkerodeite (Figure 7) are indexed only by the $P\bar{3}m1$ $Pt_4Tl_2Te_6$-type structure of synthetic $Pd_2HgSe_3$ [6] and jacutingaite $Pt_2HgSe_3$ [7]. The patterns give a best fit by a scaled cell from endmember cells of $Pd_2HgSe_3$ [6] and $Pt_2HgSe_3$ [7] based on its empirical formula, with a mean angular deviation of 0.45–0.50°, revealing the cell parameters: $a = 7.325(9)$ Å, $c = 5.288(6)$ Å, $V = 245.7(9)$ Å$^3$, and $Z = 2$. The general error of lattice parameters was estimated from its EBSD indexing cell.
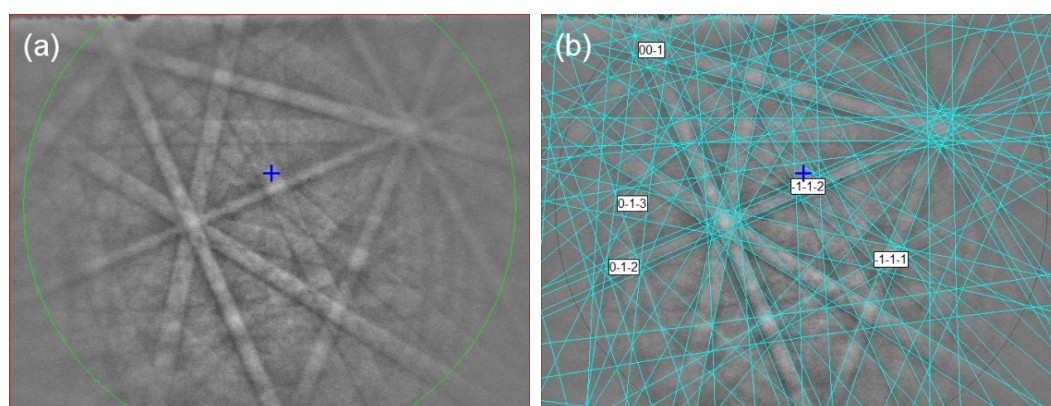


**Figure 7.** (**a**) Electron back-scatter diffraction (EBSD) pattern of one tilkerodeite crystal shown in Figure 5; (**b**) the pattern indexed with the $P\bar{3}m1$ $(Pd,Pt)_2HgSe_3$ structure.

X-ray powder diffraction data (Table 2, in Å for Cu$K\alpha1$, Bragg-Brentano geometry) were calculated from the cell parameters of tilkerodeite, atomic coordinates of synthetic $Pd_2HgSe_3$ [6], and the temperature factors of jacutingaite $Pt_2HgSe_3$ [7], with a formula of $(Pd_{1.17}Pt_{0.83})HgSe_3$ (simplified from the empirical formula in this study), using Powder Cell version 2.4 [8].

**Table 2.** Calculated X-ray powder diffraction data for tilkerodeite ($I_{rel} > 1$).

| h | k | l | d [Å] | $I_{rel}$ | h | k | l | d [Å] | $I_{rel}$ |
|---|---|---|-------|-----------|---|---|---|-------|-----------|
| 1 | 0 | 0 | 6.3436 | 6 | 4 | 1 | 0 | 1.3843 | 1 |
| 0 | 0 | 1 | 5.2880 | 9 | 0 | 4 | 2 | 1.3600 | 2 |
| 0 | 1 | 1 | 4.0618 | 8 | 4 | 0 | 2 | 1.3600 | 10 |
| 1 | 1 | 0 | 3.6625 | 6 | 3 | 0 | 3 | 1.3540 | 1 |
| 2 | 0 | 0 | 3.1718 | 2 | 0 | 3 | 3 | 1.3540 | 1 |
| 1 | 1 | 1 | 3.0109 | 9 | 4 | 1 | 1 | 1.3392 | 1 |
| **2** | **0** | **1** | **2.7200** | **100** | 1 | 4 | 1 | 1.3392 | 1 |
| 0 | 1 | 2 | 2.4405 | 5 | 0 | 0 | 4 | 1.3220 | 1 |
| 1 | 0 | 2 | 2.4405 | 4 | 0 | 1 | 4 | 1.2942 | 1 |
| 2 | 1 | 0 | 2.3977 | 1 | 3 | 2 | 2 | 1.2750 | 1 |
| 1 | 2 | 1 | 2.1837 | 4 | 2 | 3 | 2 | 1.2750 | 1 |
| 3 | 0 | 0 | 2.1146 | 2 | 2 | 2 | 3 | 1.2700 | 10 |
| **0** | **2** | **2** | **2.0309** | **34** | 1 | 3 | 3 | 1.2452 | 2 |
| 2 | 0 | 2 | 2.0309 | 6 | 1 | 1 | 4 | 1.2435 | 3 |
| 3 | 0 | 1 | 1.9634 | 2 | 2 | 0 | 4 | 1.2203 | 2 |
| 0 | 3 | 1 | 1.9634 | 1 | 0 | 2 | 4 | 1.2203 | 1 |
| **2** | **2** | **0** | **1.8313** | **37** | 3 | 3 | 1 | 1.1895 | 1 |
| 1 | 2 | 2 | 1.7761 | 5 | 4 | 0 | 3 | 1.1790 | 1 |
| 2 | 1 | 2 | 1.7761 | 3 | **4** | **2** | **1** | **1.1692** | **15** |
| 0 | 0 | 3 | 1.7627 | 5 | 1 | 2 | 4 | 1.1577 | 1 |
| 3 | 1 | 0 | 1.7594 | 1 | 5 | 0 | 2 | 1.1439 | 1 |
| 2 | 2 | 1 | 1.7304 | 3 | 3 | 2 | 3 | 1.1223 | 2 |
| 1 | 0 | 3 | 1.6983 | 3 | 0 | 3 | 4 | 1.1210 | 1 |
| 3 | 1 | 1 | 1.6694 | 2 | 3 | 0 | 4 | 1.1210 | 1 |
| 1 | 1 | 3 | 1.5883 | 3 | 1 | 5 | 1 | 1.1138 | 1 |
| 0 | 2 | 3 | 1.5407 | 4 | 2 | 4 | 2 | 1.0918 | 9 |
| **0** | **4** | **1** | **1.5191** | **19** | 4 | 2 | 2 | 1.0918 | 1 |
| 1 | 3 | 2 | 1.4648 | 2 | 4 | 1 | 3 | 1.0887 | 1 |
| 3 | 1 | 2 | 1.4648 | 2 | 1 | 4 | 3 | 1.0887 | 1 |
| 3 | 2 | 0 | 1.4553 | 1 | 2 | 2 | 4 | 1.0719 | 2 |
| 2 | 1 | 3 | 1.4202 | 3 | 6 | 0 | 0 | 1.0573 | 6 |
| 2 | 3 | 1 | 1.4032 | 1 |  |  |  |  |  |

*Note:* The strongest diffraction lines are given in bold.

## 4. Discussion

### 4.1. Relation to Other Species

An unknown mineral of the presumed composition $Pd_2HgSe_3$ (no analytical data provided) has been reported from Hope's Nose, Torquay, Devon, UK [9]. It is associated with gold, chrisstanleyite, and several other selenium species and coded as UM1998-//-Se:HgPd in the IMA-CNMNC list of unvalid unnamed minerals [10].

Tilkerodeite constitutes the Pd-analogue of jacutingaite, ideally $Pt_2HgSe_3$. Table 3 summarizes structural data for both species. Type jacutingaite from the Cauê iron-ore deposit, Itabira district, Minas Gerais, Brazil, is associated with athenite $Pd_2(As_{0.75}Hg_{0.25})$, potarite PdHg, and hematite and has the mean empirical formula $(Pt_{1.46}Pt_{0.42}Cu_{0.10}Ag_{0.01})_{\Sigma21.99}Hg_{0.98}Se_{3.04}$. Tilkerode is the second reported occurrence of jacutingaite, and the first reported occurrence of this species in original host rock assemblage.

**Table 3.** Comparative data for tilkerodeite and jacutingaite.

| Mineral/Phase | Tilkerodeite | Synthetic Pd$_2$HgSe$_3$ | Jacutingaite |
|---|---|---|---|
| formula | (Pd,Pt)$_2$HgSe$_3$ | Pd$_2$HgSe$_3$ | Pt$_2$HgSe$_3$ |
| crystal system | trigonal | trigonal | trigonal |
| space group | $P\bar{3}m1$ | $P\bar{3}m1$ | $P\bar{3}m1$ |
| $a$ [Å] | 7.325(9) | 7.3096(2) | 7.3477(2) |
| $c$ [Å] | 5.288(6) | 5.2829(1) | 5.2955(1) |
| $V$ [Å$^3$] | 245.7(9) | 244.45(1) | 247.59(1) |
| Z | 2 | 2 | 2 |
| intense XRD lines [$d$ in Å ($I$) $hkl$] | | 5.2831 (15) 001 | 5.2917 (100) 001 |
| | 2.7200 (100) 201 | 2.7151 (100) 201 | 2.7273 (16) 201 |
| | | 2.4376 (23) 012 | 2.4443 (10) 012 |
| | 2.0309 (34) 022 | 2.0280 (53) 022 | 2.0349 (18) 022 |
| | 1.8313 (37) 220 | 1.8274 (29) 220 | |
| | | | 1.7653 (37) 003 |
| | 1.5191 (19) 041 | 1.5160 (15) 041 | |
| | 1.3600 (10) 402 | | |
| | | | 1.3240 (11) 004 |
| | 1.2700 (10) 223 | 1.2681 (11) 223 | |
| | 1.1692 (15) 421 | 1.1668 (13) 421 | |
| | | | 1.0449 (11) 025 |
| reference | this paper | [6] | [7] |

### 4.2. Origin

A comprehensive discussion of the formation of the Pd–Pt–Hg–Pb–Sb–Se mineral assemblage at Tilkerode will be the subject of a companion paper. Here, we will focus on the origin of just tilkerodeite.

The presence of tilkerodeite in association with, or even inside, tiemannite suggests that both species are genetically related. Preliminary electron-probe microanalyses conducted in inclusion-poor domains of the associated tiemannite infers concentrations up to 0.4 wt. % Pd and 0.3 wt. % Pt, respectively. Thus, fluid-induced alteration of Pd–Pt-bearing tiemannite may have mobilized the PGE, which subsequently were re-deposited as tilkerodeite and jacutingaite via dissolution–reprecipitation reaction. The question of whether the amounts of PGE contained in HgSe were sufficient to account for all the tiny but numerous grains of both species cannot yet be conclusively answered.

The physico-chemical conditions during tilkerodeite formation are not properly constrained. The new species is most likely a secondary mineral and associated clausthalite and tiemannite have large stability fields in terms of temperature and relative selenium–sulfur fugacities. Thermodynamic data for the associated PGE species are lacking, as is the occurrence of T-critical minerals within the assemblage.

**Author Contributions:** C.M. performed the SEM, EBSD, and EPMA-WDS analyses and discovered the new mineral. H.-J.F. supervised the research and conducted the EPMA-EDS work. G.G. manufactured the polished sections and took care of the physical and optical data. G.G. was the first who noted the presence of jacutingaite as "unknown" species in the holotype section. H.-J.F., C.M., and G.G. wrote the paper. All authors have read and agreed to the published version of the manuscript.

**Conflicts of Interest:** The authors declare no conflict of interest.

## References

1. Tischendorf, G. Zur Genesis einiger Selenidvorkommen, insbesondere von Tilkerode im Harz. *Freib. Forsch-Hefte* **1959**, *69*, 1–168.
2. Stanley, C.J.; Criddle, A.J.; Förster, H.-J.; Roberts, A.C. Tischendorfite, $Pd_8Hg_3Se_9$: A new mineral from Tilkerode, Harz Mountains, Germany. *Canad. Miner.* **2002**, *40*, 739–745. [CrossRef]
3. Ma, C.; Rossman, G.R. Barioperovskite, $BaTiO_3$, a new mineral from the Benitoite Mine, California. *Amer. Miner.* **2008**, *93*, 154–157. [CrossRef]
4. Ma, C.; Rossman, G.R. Tistarite, $Ti_2O_3$, a new refractory mineral from the Allende meteorite. *Amer. Miner.* **2009**, *94*, 841–844. [CrossRef]
5. Armstrong, J.T. CITZAF: A package of correction programs for the quantitative electron microbeam X-ray analysis of thick polished materials, thin films, and particles. *Microbeam Anal.* **1995**, *4*, 177–200.
6. Laufek, F.; Vymazalová, A.; Drábek, M. Powder diffraction study of $Pd_2HgSe_3$. *Powder Diffr.* **2017**, *32*, 244–248. [CrossRef]
7. Vymazalová, A.; Laufek, F.; Drábek, M.; Cabral, A.R.; Haloda, J.; Sidorinová, T.; Lehmann, B.; Galbiatti, H.F.; Drahokoupil, J. Jacutingaite, $Pt_2HgSe_3$, a new platinum-group mineral species from the Cauê iron-ore deposit, Itabira District, Minas Gerais, Brazil. *Canad. Miner.* **2012**, *50*, 431–440. [CrossRef]
8. Kraus, W.; Nolze, G. POWDER CELL—A program for the representation and manipulation of crystal structures and calculation of the resulting X-ray powder patterns. *J. Appl. Crystall.* **1996**, *29*, 301–303. [CrossRef]
9. Paar, W.H.; Roberts, A.C.; Criddle, A.J.; Topa, D. A new mineral, chrisstanleyite, $Ag_2Pd_3Se_4$, from Hope's Nose, Torquay, Devon, England. *Mineral. Mag.* **1998**, *62*, 257–264. [CrossRef]
10. Smith, D.G.W.; Nickel, E.H. A system for codification for unnamed minerals: Report of the Subcommittee for Unnamed Minerals of the IMA Commission on New Minerals, Nomenclature and Classification. *Canad. Mineral.* **2007**, *45*, 983–1055. [CrossRef]